

Layered effects on soil displacement around a penetrometer

Pin-Qiang Mo^{a,*}, Alec M. Marshall^b, Hai-Sui Yu^c

^a*State Key Laboratory for GeoMechanics and Deep Underground Engineering, China University of Mining and Technology, China. E-mail: pinqiang.mo@cumt.edu.cn*

^b*Faculty of Engineering, University of Nottingham, UK. E-mail: alec.marshall@nottingham.ac.uk*

^c*School of Civil Engineering, University of Leeds, UK. E-mail: PVC.int@leeds.ac.uk*

Abstract

The interpretation of cone penetration test (CPT) data is important for the in-situ characterisation of soils. Interpretation of CPT data remains a predominately empirical process due to the lack of a rigorous model that can relate soil properties to penetrometer readings. Interpretation is especially difficult in layered soils, where penetrometer response can be affected by several horizons of soil with different properties. This paper aims to provide some insight into the mechanisms of soil displacement that occur as a penetrometer is pushed into layered soils. Data is presented from centrifuge modelling of probe penetration in layered soils in an axisymmetric container where soil deformation patterns around the probe can be measured. Results obtained from uniform soil tests are also presented to illustrate the effects of soil density and stress level (i.e. centrifuge acceleration). A large influence zone is found to relate to the higher penetration resistance obtained in a denser soil. Differing soil displacement patterns at low and high stresses are

*Corresponding author

related to the tendency of the soil to dilate, with the well-known consequence of a non-linear increase of penetration resistance with stress level. Layered soil tests show a clear difference of soil deformation patterns compared to uniform tests, especially for vertical displacements. The peak value of vertical displacement of the soil occurs at dense-over-loose interfaces, while a local minima occurs at loose-over-dense interfaces. Parameters are proposed to quantitatively evaluate the layered effects on soil deformations and a deformation mechanism is described for penetration in layered soils based on the transition of displacement profiles.

Keywords: cone penetration test, soil displacement, layered effect

1. Introduction

Cone penetration tests (CPT) are frequently used in geotechnical engineering for in-situ evaluations of soil properties and profiles. CPT data is also valuable for use within pile design methods and for the evaluation of soil liquefaction potential. The response of a CPT is very complex; it relates not only to the mechanical properties of the soil in which the probe tip is penetrating, but also the properties and proximity of nearby horizons of soil. As such, rigorous analysis of CPT data is very difficult and interpretation generally relies on empirical relationships for soil identification and classification (Sadrekarimi, 2016).

The CPT probe generates a complex deformation field as it penetrates into the soil. For plane-strain conditions, a comprehensive illustration of soil patterns around a flat-bottomed penetrometer was provided by White (2002) and White and Bolton (2004). The tests were conducted at 1-g ($g = \text{grav}$ -

ity) within a pressure chamber, and the results include streamlines of soil movement and stress profiles at the base of the penetrometer. The evolution of soil element deformation was illustrated and the reduction of stresses above the pile tip was related to cavity contraction caused by the densification of soil around the shaft. Mo (2014) reported results from axisymmetric elevated-g tests using a geotechnical centrifuge in which a half-cylindrical probe with a conical tip was pushed along a Perspex wall into both uniform and layered soil profiles. A resistance ratio was proposed in order to evaluate the transition curve of penetration resistance as the probe moved from one soil layer to another. A fully three-dimensional investigation was achieved by Paniagua et al. (2013) by using digital image correlation on x-ray microtomography data. The authors were able to evaluate deformations around a fully-cylindrical penetrometer pushed into pressurised samples of silt. Failure patterns were described from the evolution of volumetric and shear strains.

Natural soil deposits often consist of layers with varying thickness and mechanical properties. Gui and Bolton (1998) reported that the CPT profile in layered soils deviates from a uniform soil profile when the probe reaches a certain distance from the soil layer interface and that some distance is required to develop a new tip resistance once the probe has penetrated into the second soil layer. Thus the transition zone around the soil layer interface can be separated into two parts: (1) the transition zone above the interface in which the probe begins to sense the underlining soil layer, and (2) the transition zone below the interface which extends to the depth where the probe is no longer influenced by the upper soil layer. Transition zones around soil layer interfaces have been shown to depend on the properties and thickness

40 of soil layers (Meyerhof and Sastry, 1978a,b; Youd and Idriss, 2001; Mo et al.,
41 2015). Analytical methods (e.g. Vreugdenhil et al., 1994; Mo et al., 2017)
42 and numerical approaches (e.g. Ahmadi and Robertson, 2005; Xu, 2007;
43 Walker and Yu, 2010) have also been performed to investigate penetration
44 problems in layered soils. Despite these valuable contributions, there is still
45 a limited amount of data available on penetration induced soil deformations
46 within layered soils.

47 In this paper, data obtained from geotechnical centrifuge modelling of
48 cone penetration tests in layered soils are included, with a particular em-
49 phasis on the illustration of soil deformations around the probe. The exper-
50 imental equipment is the same as that presented in Mo et al. (2015); the
51 penetrometer consisted of a half-cylindrical probe with a conical tip which
52 was pushed into the soil at a Perspex wall in an axisymmetric container,
53 thereby enabling the measurement of subsurface soil movements using dig-
54 ital image analysis. The paper first discusses the effect of soil density and
55 stress level effect on deformation patterns. This is followed by a detailed
56 illustration of the effect of soil layering on soil deformation patterns. The
57 paper supplements the work presented in Mo et al. (2015) and Mo et al.
58 (2017) in several ways: (1) additional results are presented that relate to the
59 effects of stress condition; (2) the method for interpreting layered effects on
60 soil displacements is elaborated; (3) profiles of displacements after penetra-
61 tion are presented which indicate different mechanisms for a loose-over-dense
62 compared to a dense-over-loose configuration of soil layers; and (4) transition
63 parameters of both horizontal and vertical displacements are introduced to
64 quantitatively evaluate the layered effects on soil displacements, which are

65 also related to the transitions based on penetration resistance.

66 **2. Centrifuge tests and soil deformation measurement**

67 Centrifuge tests were conducted using Fraction E silica sand (mean grain
68 size $d_{50} = 0.14$ mm) with layers of varying relative density in a 180° axisym-
69 metric model. Tests were performed on the Nottingham Centre for Geome-
70 chanics (NCG) 2 m radius geotechnical centrifuge. The penetrometer had a
71 diameter of $B = 12$ mm and was pushed into the sand at a speed of 1 mm/s.
72 Soil models were prepared by the multiple-sieving air pluviation method (Mo
73 et al., 2015) to either a relatively dense state with relative density (D_r) of
74 approximately 90 % or a relatively loose state with relative density of approx-
75 imately 50 %. Note that the relatively loose sand, referred to simply as loose
76 in this paper, falls within the ‘medium dense’ range ($D_r = 35 \% \sim 65 \%$),
77 and the relatively dense sand, referred to as dense, falls within the ‘very
78 dense’ range ($D_r = 85 \% \sim 100 \%$), based on *BS EN ISO 14688 – 2 : 2004*.
79 Tests were performed at both 50 *g* (centrifuge acceleration) and 1 *g* to evalu-
80 ate the effects of stress level. Note that at prototype scale, the penetrometer
81 represents a 0.6 *m* diameter pile, which is comparable to a typical full-scale
82 driven pile. The comparison between 50 *g* and 1 *g* results aims to provide
83 an indication of the effect of stress condition on the induced soil deformation
84 mechanism. Details of the layered soil profiles are summarised in Table 1.

85 A half-cylindrical model container with a Perspex window was used to en-
86 able the observation of penetration-induced sub-surface soil deformations, as
87 shown in Figure 1(a). Digital cameras were used to obtain a series of images
88 of the penetrometer and soil throughout the tests. Soil deformations caused

Table 1: Details of soil profiles for centrifuge tests

Test ID	Soil Layer Details	Depth of Soil 1 (mm)	Depth of Soil 2 (mm)	Depth of Soil 3 (mm)	Total depth (mm)
T01-1g	D	297	-	-	297
T02	D	301	-	-	301
T03	L	298	-	-	298
T04	L/D	85	205	-	290
T05	D/L	97	201	-	298
T06	L/D/L	87	65	142	294
T07	D/L/D	90	57	153	300

‘D’: dense sand ($D_r \approx 90\%$); ‘L’: loose sand ($D_r \approx 50\%$);

‘L/D’: loose over dense layers; Soil 1 is upper soil.

89 by the penetrometer, schematically presented in Figure 1(b), were measured
90 using the Matlab-based image analysis methodology ‘geoPIV’ developed by
91 White et al. (2003). Note that ‘ X ’ and ‘ Y ’ represent the horizontal and
92 vertical positions of soil elements, and ‘ Δx ’ and ‘ Δy ’ indicate horizontal and
93 vertical displacements, respectively. ‘ H ’, defined as $H = z - z_{interface}$, in-
94 dicates the distance between the cone shoulder and the soil layer interface.
95 The upper soil layer interface is taken as the location of $z_{interface}$ (Figure 1b)
96 to define H for multi-layered tests. Further details on test set-up and proce-
97 dures can be found in Mo (2014).

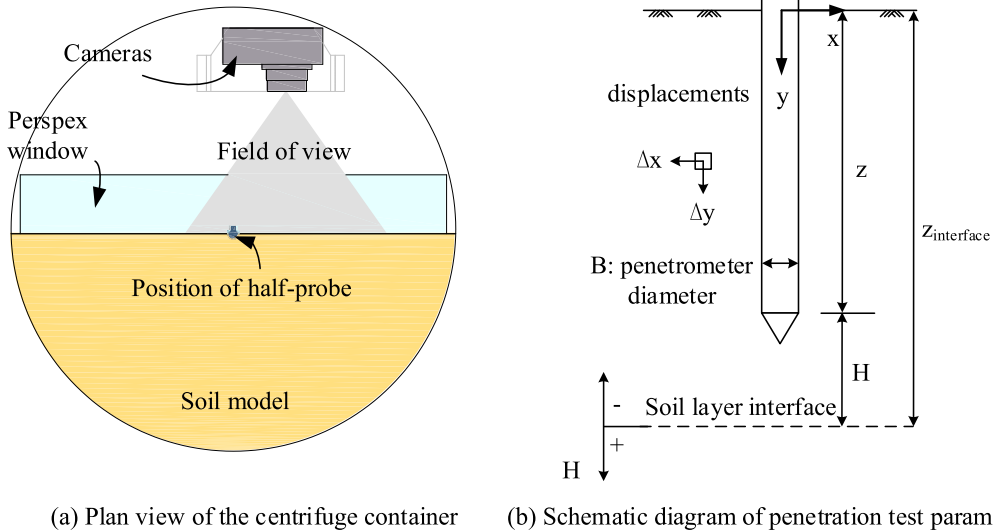


Figure 1: Centrifuge tests: (a) Plan view of the centrifuge container; (b) Schematic diagram of penetration test parameters

98 3. Results and Discussion

99 3.1. Effects of soil density

100 It has been demonstrated that the response of a penetrometer in granu-
 101 lar soils is dominated by two factors: confining stress and soil density (e.g.
 102 Lee, 1990; Bolton et al., 1999; Mo, 2014). In a granular soil, as the probe
 103 advances into the soil, the particles are pushed outwards to accommodate
 104 the probe and are simultaneously dragged downwards owing to shearing at
 105 the soil-probe interface. The soil around the probe is compressed and confin-
 106 ing stresses in the soil increase, which in turn act on the probe and increase
 107 the penetration resistance. Results from the uniform soil tests T02 and T03
 108 can be used to illustrate the effects that soil relative density and penetration
 109 depth have on deformation patterns. Figure 2 presents the profiles of nor-

110 malised cumulative displacement ($2 \Delta x/B, 2 \Delta y/B$) after 160 mm of penetra-
111 tion for soil elements located at varying normalised offsets ($2 X/B = 2 \rightarrow 6$)
112 from the penetrometer in tests T02 and T03. The figure shows the relative
113 radial (Δy on the left-side of the plots) and axial (Δx on the right-side)
114 displacements that occurred within the soil. The deformation fields for the
115 dense and loose tests are similar, though deformations extend further away
116 from the probe and surface heave ($-\Delta y$) is more obvious in the dense sand
117 test. Additionally, strains calculated based on the soil displacement data
118 showed that the loose sand close to the probe experienced larger volumetric
119 strains owing to the greater compressibility and less restricted dilation (Mo,
120 2014).

121 The movement of a soil element near the probe is initially predominately
122 downwards, but becomes increasingly outwards as the probe approaches, ul-
123 timately reaching a similar vertical and horizontal movement (White and
124 Bolton, 2004; Liu, 2010; Mo et al., 2015). As a result, penetration leads to
125 a cylindrical deformation zone around the probe shaft and a spherical defor-
126 mation region ahead of the cone, as shown in the cumulative displacement
127 profiles in Figures 2 and 3. For soil around the probe shaft, the reduction of
128 displacement with offset from the penetrometer implies that the observable
129 lateral influence zone is about $5 B$ wide for dense sand, and approximately
130 $3.5 B$ for loose sand, based on the results from Mo et al. (2015). Note that
131 this influence zone is defined based on the PIV displacement data (i.e. the
132 zone where the PIV technique was able to measure displacements caused
133 by penetration) and does not define the distance required to a boundary
134 required to avoid boundary effects. For the same tests, the value of cone

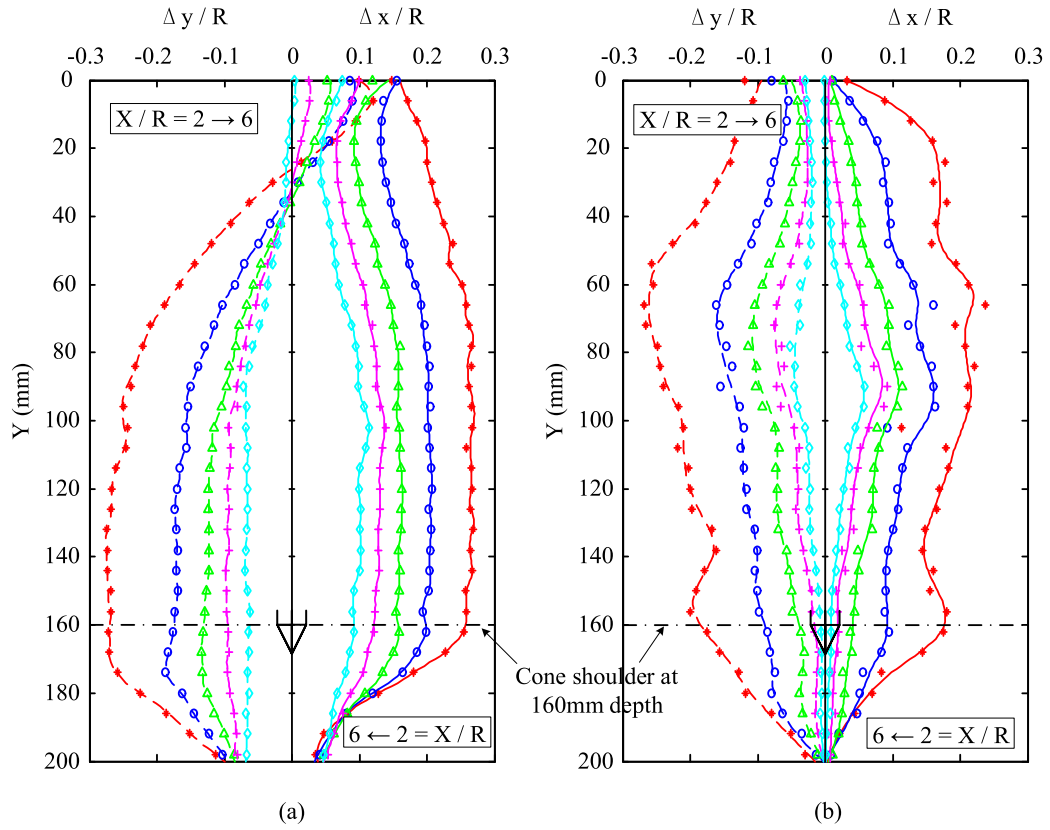


Figure 2: Cumulative displacement profiles after 160 mm of penetration: (a) dense sand: T02; (b) loose sand: T03

135 tip resistance in the dense sand was found to be about 2 – 3 times that for
 136 the loose sand. There is certainly a link between observed soil displacement
 137 patterns and penetration resistance, though this data indicates that it is not
 138 a simple linear relationship.

139 3.2. Effects of stress level

140 The uniform dense sand tests at different g-levels (T01: 1 g and T02:
 141 50 g) can be used to demonstrate the effects of stress level on data obtained

142 from penetration tests. The magnitude of penetration resistance of the 50 g
143 test was found to be 10 – 12 times greater than that from the 1 g test (Mo,
144 2014), indicating that the penetration resistance does not scale linearly with
145 g-level (as demonstrated by Bolton et al., 1999). In order to illustrate the
146 effects of initial stress level (i.e. centrifuge acceleration) on soil deformations,
147 Figure 3 provides contours of cumulative and instantaneous total displace-
148 ments ($\sqrt{\Delta x^2 + \Delta y^2}$) for both the 50 g and 1 g tests. The total displacement
149 after 120 mm of penetration from the 1 g test shows a slightly larger defor-
150 mation zone as well as more pronounced heaving near the surface. Similar
151 trends are also shown in the instantaneous contours ($\Delta z = 6$ mm in subplots
152 (c) and (d) represents an interval of penetration distance), where the heaving
153 effect in the 50 g test is more constrained by the higher stress levels.

154 From the results of the 1 g test, the larger deformation contours, espe-
155 cially for the soil near the surface, indicate the higher volumetric strains that
156 are a consequence of the increased tendency of the soil to dilate under lower
157 confining stresses (compared to the 50 g test). The instantaneous total dis-
158 placement vectors also show that the soil is displaced more outwards and
159 upwards in the 1 g test, indicating the dilatant behaviour induced by the
160 shearing around the cone. The larger deformation zone in the 1 g test would
161 therefore create a relatively higher stress state around the probe in the 1 g
162 test compared to the 50 g test. Thus the ratio between the cone tip resistance
163 and the in-situ stress condition (q_c/p'_0) would decrease as the stress level is
164 increased (i.e. from the 1 g to 50 g test), which has been reported as a typical
165 phenomenon for cone penetration tests from both field and laboratory trials
166 (Jamiolkowski et al., 1988; Bolton et al., 1999).

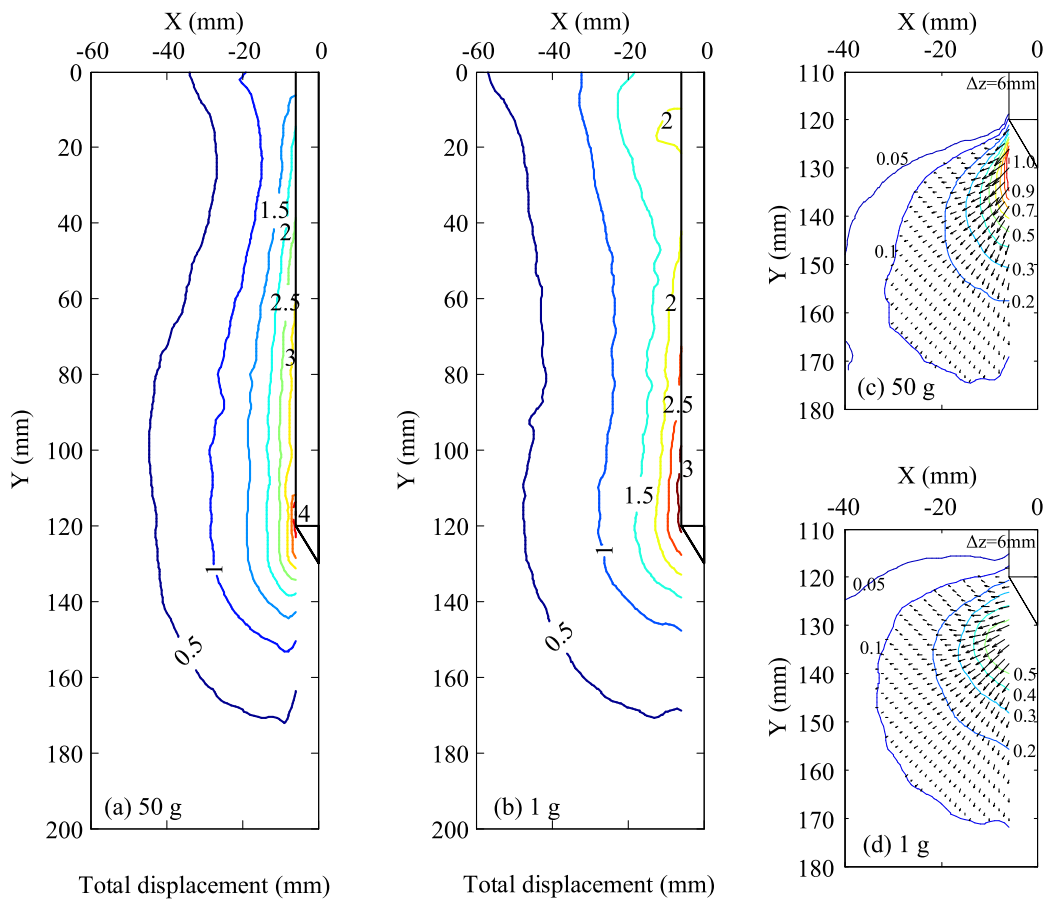


Figure 3: Contours of total displacements after 120 mm of penetration in dense sand: cumulative displacements (in mm): (a) 50 g, (b) 1 g; instantaneous displacements (in mm): (c) 50 g, (d) 1 g

167 *3.3. Layered effects on soil displacements*

168 This section considers the displacement data from the layered soil cen-
169 trifuge tests. The transition of penetration resistance in two-layered soil tests
170 is presented in Figure 4a. A cone tip resistance ratio η' was defined by Mo
171 (2014) as

$$\eta' = \frac{q_c - q_{c,w}}{q_{c,s} - q_{c,w}} \quad (1)$$

172 where $q_{c,w}$ and $q_{c,s}$ are the resistance in the uniform weak (loose) and strong
173 (dense) soils, respectively. The trend of η' tracks the transition of cone tip
174 resistance q_c when penetrating in layered soils and varies from 0 in a relatively
175 weak soil layer to 1 in a relatively strong layer. The expression

$$\eta'_{fit} = \frac{1}{1 + S_1 \times \exp(S_2 \times H/B)} \quad (2)$$

176 can be fitted to the η' data from the two-layered tests in Figure 4a, where H is
177 the distance to the soil layer interface normalised by penetrometer diameter
178 B (Figure 1) and S_1 , S_2 are curve fitting parameters. When the probe is
179 pushed from loose into dense sand (T04), η' transforms from 0 to 1, and the
180 transition zone is larger in the dense layer ($4B$) compared to the loose sand
181 ($2B$). For the tests where the probe goes from dense sand to loose sand
182 (T05), the transition zone is again larger in the dense sand ($5B$) than in the
183 loose sand ($1B$).

184 Figure 5 shows the profiles of normalised cumulative displacement in the
185 two-layered tests (T04-T05), which illustrate a considerable curvature in the
186 profiles of displacements around the location of the layer interface between
187 the loose and dense soils. For the test with loose over dense sand (T04),

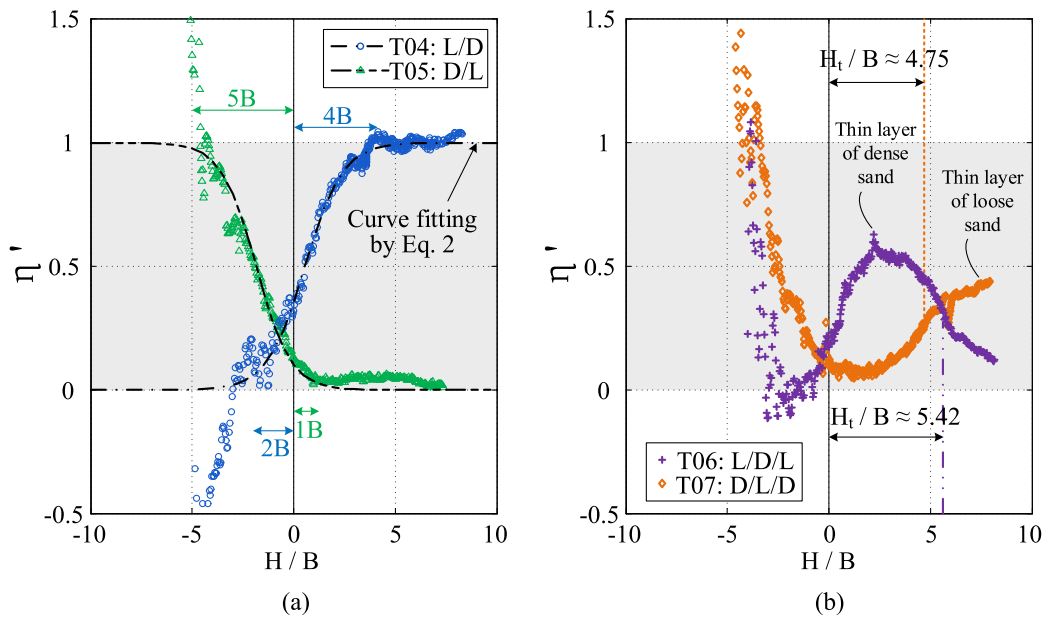


Figure 4: Layered effects on penetration resistance: (a) two-layered soils; (b) three-layered soils

188 the transition zone in the loose soil is around $2B$ based on the profile of
189 $2\Delta y/B$, where the penetration resistance starts to be affected, as shown in
190 Figure 4a. This agrees with the extent of the transition zone based on η' in
191 Figure 4a. A local minimum of $2\Delta y/B$ occurs at the loose-dense interface,
192 followed by the gradual increase of vertical displacement as the probe pushes
193 into the dense soil. The extent of the transition zone in the dense soil is not
194 clear from this data. A slight increase of horizontal displacements occurs at
195 the transition from loose to dense sand layer, however the transition zones
196 around the layer interface are not clear based on the Δx data.

197 For the test with dense over loose sand (T05), by comparing the data in
198 Figure 5b with those in Figure 2a, it can be seen that the vertical displace-
199 ments occurring when the probe approaches the layer interface are larger in
200 the layered test compared to those at an equivalent depth in the uniform
201 dense test. The peak displacement of $2\Delta y/B$ occurs at the dense-over-loose
202 interface, and the transition zone in the loose sand is about $4B$ based on
203 vertical displacements. This is much larger than the value of $1B$ observed
204 from the resistance transition curve in Figure 4a. Again, there is a small
205 change (decrease) of horizontal displacement from dense to loose sand layer,
206 but this data can not be used to identify the extent of a transition zone.

207 Similar trends can also be found for tests T06 and T07 (Figure 6), where
208 a thin layer of dense or loose sand is sandwiched between layers of loose
209 or dense sand, respectively. The observation confirms that the peak value
210 of vertical displacements occurs at the dense-over-loose interface, whereas a
211 local minimum occurs at the loose-over-dense interface.

212 Figure 7 shows the locations (based on measured displacements) of the soil

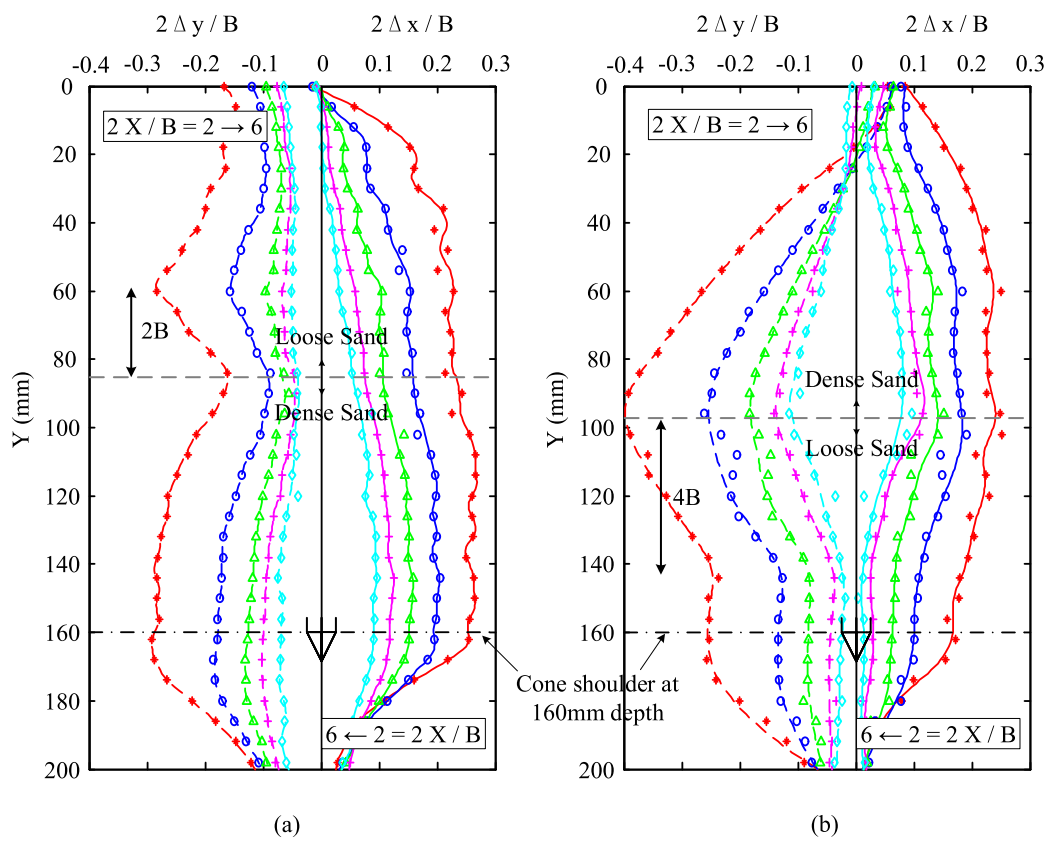


Figure 5: Cumulative displacement profiles after 160 mm of penetration: (a) loose over dense T04; (b) dense over loose T05

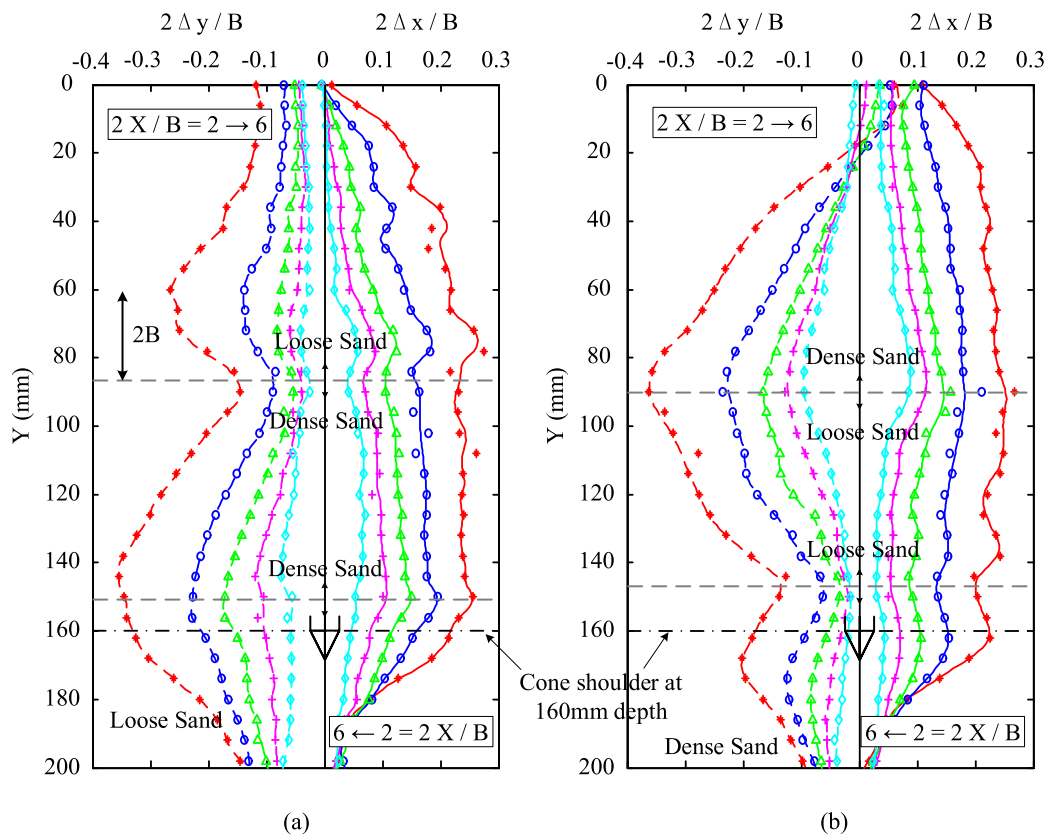


Figure 6: Cumulative displacement profiles after 160 mm of penetration: (a) dense sand-sandwiched between loose T06; (b) loose sand sandwiched between dense T07

213 layer interface during the layered tests after 160 mm of penetration. Included
214 in the plots are data from the uniform dense (T02) and loose (T03) tests based
215 on displacements at depths corresponding to the locations of the interfaces
216 in the layered tests. The displacements from the uniform tests are similar for
217 the dense and loose sand at shallower depths ($Y = 85$ to 98 mm in plots a,
218 b, c-1 and d-1) but differ slightly at deeper locations ($Y \approx 150$ mm in plots
219 c-2 and d-2), where the dense sand experiences greater displacements.

220 The displacements from the layered tests are shown to fall outside of the
221 range of displacements from the uniform sand tests. The displacements from
222 the loose-over-dense interfaces are always less than the displacements from
223 both the uniform dense and loose tests, supporting the observation of a local
224 minimum at the layer interface in the Δy data in Figures 5 and 6. The
225 opposite is true for the dense-over-loose interfaces, where displacements are
226 greater than those from both the uniform dense and loose tests (indicating
227 a peak in Δy observed at the layer interfaces in Figures 5 and 6).

228 The data presented thus far indicate that the pattern of soil displacements
229 around the interfaces between soil layers is affected by the properties of the
230 soil in the respective layers. However, the figures have not demonstrated a
231 clear definition of the extent of the transition zones based on soil displacement
232 data. In order to better quantify the extent of the transition zones from the
233 displacement data, the approach adopted for penetration resistance (Xu and
234 Lehane, 2008; Mo, 2014) is now applied to the displacement data.

235 Following the definition of the cone tip resistance ratio η' in Equation 1
236 (plotted in Figure 4), the changes of soil deformation between layered and
237 uniform tests can be treated as a ratio, which is termed ξ' . Due to the

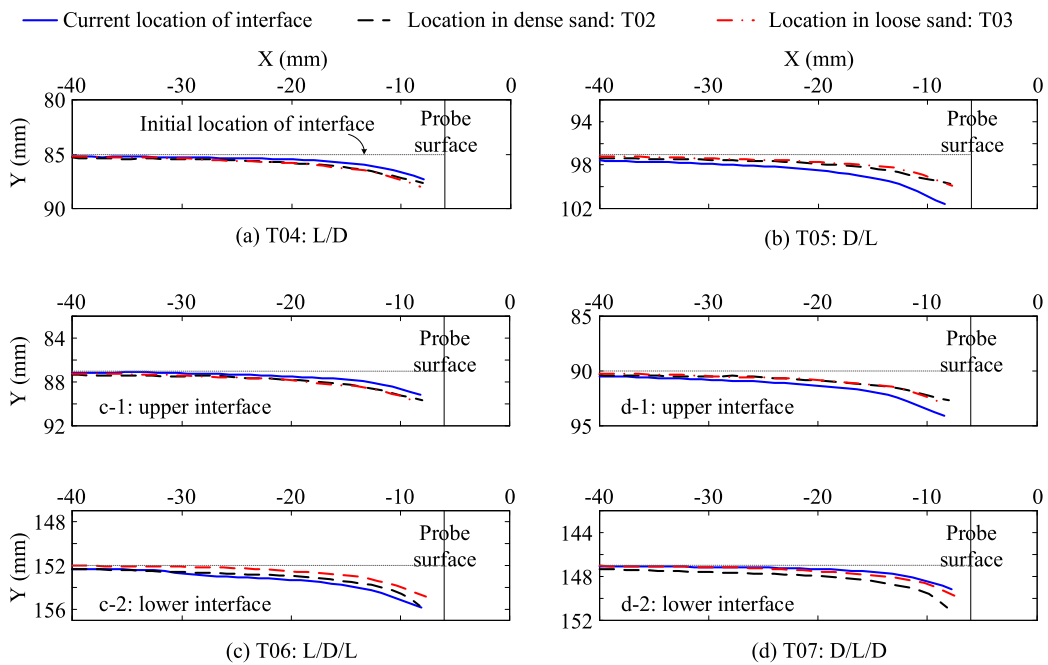


Figure 7: Displacement of soil layer interfaces after 160 mm of penetration for tests: T04-T07

238 different magnitude of the effect of soil layering on horizontal and vertical
 239 displacements, ξ' is evaluated for Δx and Δy separately as:

$$\xi'_{\Delta x} = \frac{\Delta x - \Delta x|_w}{\Delta x|_s - \Delta x|_w} \quad (3)$$

$$\xi'_{\Delta y} = \frac{\Delta y - \Delta y|_w}{\Delta y|_s - \Delta y|_w} \quad (4)$$

240 where the subscripts 's' and 'w' relate to the uniform soil tests with dense
 241 (strong) and loose (weak) sand, respectively.

242 Figure 8 considers test T04 in particular, where loose soil overlies dense
 243 soil. Calculation of ξ' was based on the cumulative displacements (Δx and
 244 Δy) after 160 mm of penetration. Displacements at an offset distance of
 245 $2X/B = 2$, illustrated in subplot (a), were used to calculate the values of
 246 $\xi'_{\Delta x}$ and $\xi'_{\Delta y}$ in subplots (b) and (c), respectively. The displacement data
 247 from the uniform dense and loose tests (T02 and T03), which are used in the
 248 calculation of ξ' , are also included in subplot (a).

249 Similar to the transition curve of η' (see Figure 4a), the transition of $\xi'_{\Delta x}$
 250 generally varies from 0 in the loose sand to 1 in the dense sand, as shown in
 251 Figure 8(b). The scatter in the $\xi'_{\Delta x}$ is rather large in the loose sand layer
 252 due to the fact that values of Δx were very similar in all of the tests (see
 253 Figure 8(a)).

254 The value of $\xi'_{\Delta y}$ also transforms from 0 to 1, but values around the layer
 255 interface range widely beyond the $0 \rightarrow 1$ limits. These values occur because
 256 of the layered soil effect on the trend of Δy in test T04 as well as the seemingly
 257 coincidental 'crossing' of the Δy data from the uniform loose and dense tests
 258 near the location of the layer interface in test T04. The magnitude of $\xi'_{\Delta y}$

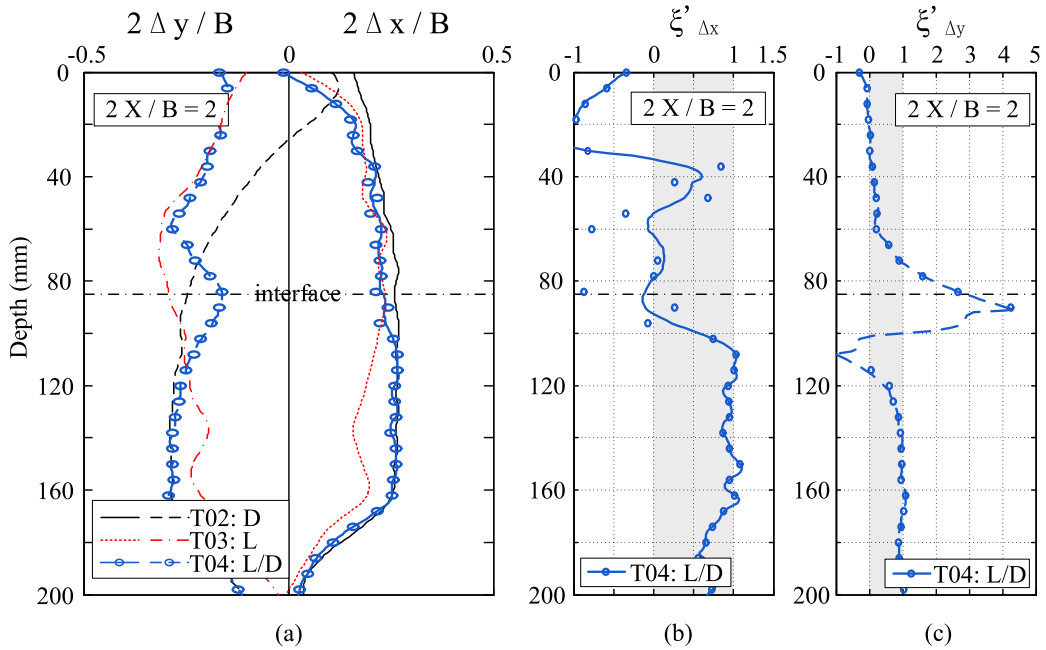


Figure 8: Layered effects on soil deformation ($2X/B = 2$) for test T04

259 increases up to approximately 4 in the soil just below the layer interface and
 260 drops dramatically to negative values at $H/B \approx 2$. Below this location,
 261 $\xi'_{\Delta y}$ increases gradually to 1 as the displacements in the layered tests begin
 262 to match those from the uniform dense test.

263 It should be noted that some results may have been affected by the prox-
 264 imity of the layer interface to the surface. At the depth of the layer interface
 265 ($\approx 80\text{mm}$), the displacements in the uniform dense and loose tests (Figure 2)
 266 appear to be affected by the ground surface (not yet reaching a steady trend).
 267 Ideally this layer interface would have been located at a deeper location.

268 Figure 9 presents the ξ' results based on displacements at the other values
 269 of lateral offsets ($2X/B = 2 \rightarrow 6$). Again, the scatter in $\xi'_{\Delta x}$ is attributed to

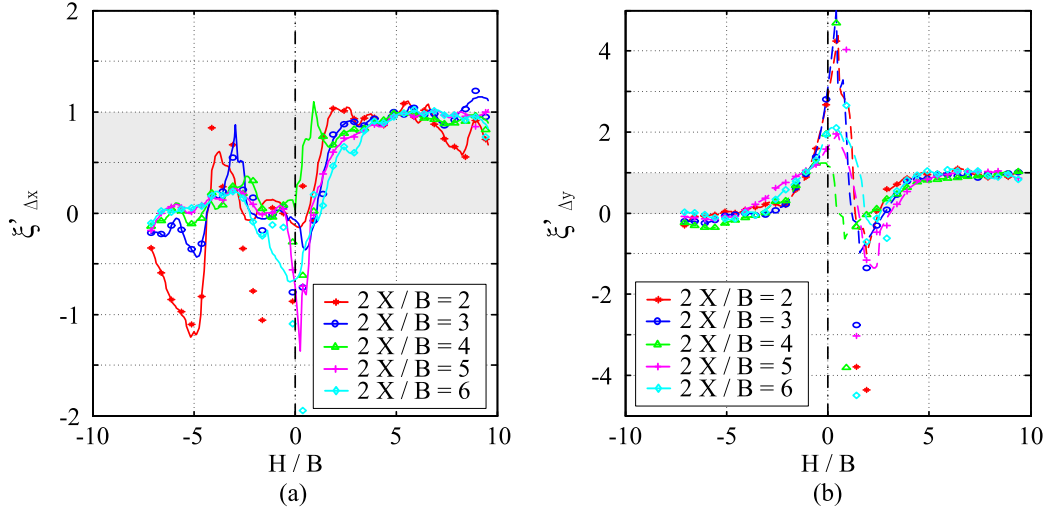


Figure 9: ξ' with variation of offset: $2X/B = 2 \rightarrow 6$ (T04)

270 the similar horizontal displacement in dense and loose sand. Data smoothing
 271 was thus applied by a method of robust local regression in Matlab, using a
 272 span of 5% of the total number of data points. The transition curves of $\xi'_{\Delta x}$
 273 and η' seem to show comparable extents of the transition zones around the
 274 soil layer interface (i.e. $2B$ in loose sand and $4B$ in dense sand for T04),
 275 though the scatter in the loose layer makes delineation of the transition zone
 276 difficult. The trend of $\xi'_{\Delta y}$ is relatively clear, with a peak value occurring
 277 adjacent to the layer interface, followed by a negative value and then levelling
 278 off towards 1. The data suggests that the offset from the penetrometer does
 279 not have a significant influence on the trend of ξ' .

280 Figure 10 shows the transition of $\xi'_{\Delta y}$ for all the layered soil tests, includ-
 281 ing two-layer (subplot a) and three-layer tests (subplot b, where H_t is the
 282 thickness of the sandwiched soil layer). Similar to the trends of η' in Figure 4,

283 the layered effects are clear, with either a drastic jump or a peak/minimum
284 around the soil layer interfaces. The thin-layer effect (from the three-layer
285 tests in Figure 10b) is shown to cause considerable fluctuations of the η' data
286 at the location of the layer interfaces. The dramatic variation of $\xi'_{\Delta y}$ near the
287 first soil layer interface may, like the data presented in Figures 8 and 10a, be
288 due to surface effects. The transition around the second soil layer interface,
289 located at a depth of ≈ 150 mm where surface effects on the uniform test
290 data (Figure 2) are insignificant, shows a more reasonable peak at the dense-
291 over-loose interface and a minimum at the loose-over-dense interface. The
292 value of $\xi'_{\Delta y}$ around the dense-over-loose interface for T06 is greater than 1,
293 indicating that the layer interface is moved vertically downwards more than
294 in the uniform sand tests. Correspondingly, the loose-over-dense interface
295 for T06 with $\xi'_{\Delta y} < 0$ indicates that vertical displacements were less than in
296 both of the uniform sand tests, confirming the phenomenon observed from
297 Figure 7.

298 The distributions of soil deformation around the penetrometer provide in-
299 sights into the mechanisms that are responsible for the probe resistance data
300 as the cone passes between soil layers. Figure 11 schematically illustrates
301 the displacement mechanisms for penetration in layered soils. For soil above
302 a loose-over-dense interface, the vertical displacements are restricted by the
303 underlying stiffer layer with lower compressibility. For the dense-over-loose
304 interface, larger vertical displacements occur owing to the cumulative den-
305 sification of the underlying, more compressible layer. Although test results
306 were somewhat affected by the proximity of the ground surface to some of
307 the layer interfaces, the effects of soil layering on trends of displacements

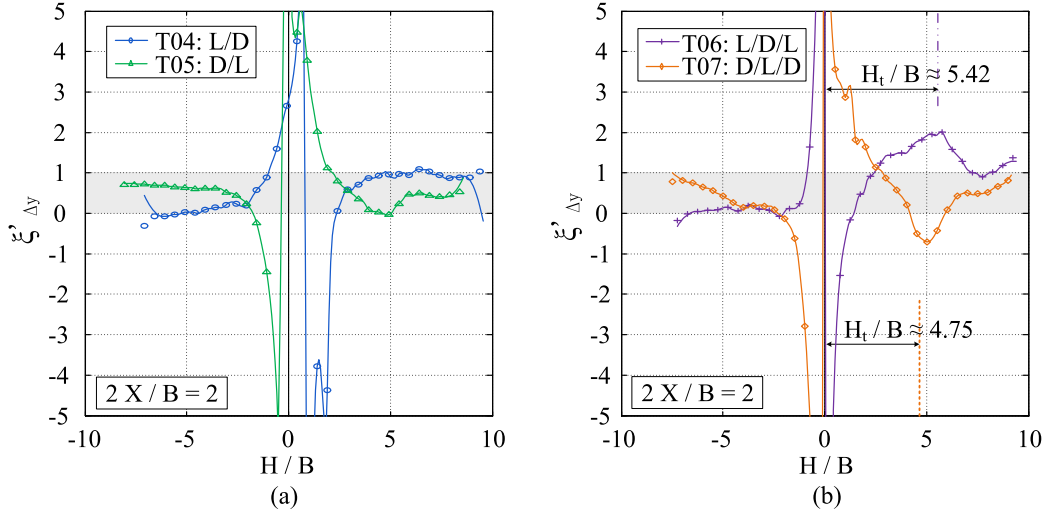


Figure 10: Layered effects on soil deformation ($2X/B = 2$) for tests with: (a) two-layered soils; and (b) three-layered soils

308 was generally clear. The observations provided in this paper may assist in
 309 the qualitative interpretation of CPT data; further work is still required to
 310 achieve a quantitative methodology for relating penetration resistance and
 311 soil deformations in layered soils. The results provided here may also provide
 312 a useful validation dataset for new developments of numerical and analytical
 313 methods for CPT data interpretation.

314 4. Conclusions

315 This paper presented data obtained from a series of centrifuge tests aimed
 316 at investigating the effects of soil layering on ground displacement mecha-
 317 nisms around the probe.

318 Data from uniform soil tests was provided as a reference to compare
 319 layered test data against. The effects of soil density and stress level were

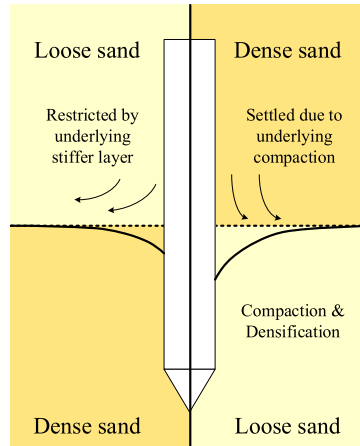


Figure 11: Schematic of displacement mechanism for penetration in layered soils

320 illustrated from the uniform test results. A large influence zone based on
 321 soil displacements was noted for the dense sand, owing to its relatively low
 322 compressibility. The large influence zone and associated higher soil stresses
 323 relates well to higher penetration resistance in the dense soil compared to
 324 the loose soil. A larger deformation zone was observed under lower stress
 325 conditions due to the increased tendency of the soil to dilate. This results in
 326 a relatively high stress state around the probe under low stress conditions,
 327 which explains the non-linear increase of penetration resistance with stress
 328 level.

329 Soil layering was shown to have a clear effect on soil deformation patterns.
 330 The change of vertical displacement profile around the soil layer interfaces
 331 was more obvious than for the horizontal displacement profile. A peak value
 332 of soil vertical displacement occurred at dense-over-loose interfaces, while
 333 a local minimum occurred at loose-over-dense interfaces. Additionally, dis-
 334 placements at loose-over-dense interfaces were less than those that occurred

335 in both the uniform dense and loose tests. For the dense-over-loose interfaces,
336 the displacements were greater than for the uniform soil tests.

337 The parameters $\xi'_{\Delta x}$ and $\xi'_{\Delta y}$ were proposed to evaluate the transition
338 of displacement profiles for penetration in layered soils. The trends of ξ'
339 provided a quantitative evaluation of the layered effects on soil deformation.
340 The transition curves of $\xi'_{\Delta x}$ and η' were noted to be comparable, with similar
341 extents of transition zones around the soil layer interface, though the scatter
342 in the $\xi'_{\Delta x}$ made conclusive delineation of transition zones difficult. The
343 trend of $\xi'_{\Delta y}$ was relatively clear, with a peak value occurring adjacent to the
344 dense-over-loose interface and a minimum at the loose-over-dense interface.
345 It was shown that the offset distance from the pile did not significantly affect
346 the profile of ξ' . A deformation mechanism for penetration in layered soils
347 was described based on the observed results from the centrifuge tests.

348 **5. Acknowledgments**

349 The authors would like to acknowledge financial support by the Funda-
350 mental Research Funds for the Central Universities (No. 2017QNB10).

351 **References**

- 352 Ahmadi, M. M., Robertson, P. K., 2005. Thin-layer effects on the CPT $q(c)$
353 measurement. *Canadian Geotechnical Journal* 42 (5), 1302–1317.
- 354 Bolton, M. D., Gui, M. W., Garnier, J., Corte, J. F., Bagge, G., Laue, J.,
355 Renzi, R., 1999. Centrifuge cone penetration tests in sand. *Géotechnique*
356 49 (4), 543–552.

- 357 Gui, M., Bolton, M. D., 1998. Geometry and scale effect in cpt and pile
358 design. In: Robertson, P., Mayne, P. (Eds.), *Geotechnical Site Character-*
359 *ization: Proceedings of the First International Conference on Site Char-*
360 *acterization, ISC'98. Vol. 2. Balkema, Rotterdam, Atlanta, Georgia, pp.*
361 *1063–1068.*
- 362 Jamiolkowski, M., Ghionna, V. N., Lancellotta, R., Pasqualini, E., 1988.
363 New correlations of penetration test for design practice. Invited Lecture.
364 In: *ISOPT-1. pp. 196–263.*
- 365 Lee, S. Y., 1990. Centrifuge modelling of cone penetration testing in cohe-
366 sionless soils. Ph.D. thesis, University of Cambridge, UK.
- 367 Liu, W., 2010. Axisymmetric centrifuge modelling of deep penetration in sand.
368 Ph.D. thesis, University of Nottingham.
- 369 Meyerhof, G. G., Sastry, V. V. R. N., 1978a. Bearing capacity of piles in
370 layered soils.1. clay overlying sand. *Canadian Geotechnical Journal* 15 (2),
371 171–182.
- 372 Meyerhof, G. G., Sastry, V. V. R. N., 1978b. Bearing capacity of piles in
373 layered soils.2. sand overlying clay. *Canadian Geotechnical Journal* 15 (2),
374 183–189.
- 375 Mo, P. Q., 2014. Centrifuge modelling and analytical solutions for the cone
376 penetration test in layered soil. Ph.D. thesis, University of Nottingham.
- 377 Mo, P. Q., Marshall, A. M., Yu, H. S., 2015. Centrifuge modelling of cone
378 penetration tests in layered soils. *Géotechnique* 65 (6), 468–481.

- 379 Mo, P. Q., Marshall, A. M., Yu, H. S., 2017. Interpretation of cone penetra-
380 tion test data in layered soils using cavity expansion analysis. *Journal of*
381 *Geotechnical and Geoenvironmental Engineering* 143 (1), 04016084–1–12.
382 DOI: 10.1061/(ASCE)GT.1943–5606.0001577.
- 383 Paniagua, P., Ando, E., Silva, M., Emdal, A., Nordal, S., Viggiani, G., 2013.
384 Soil deformation around a penetrating cone in silt. *Géotechnique Letters*
385 3, 185–191.
- 386 Sadrekarimi, A., 2016. Evaluation of cpt-based characterization methods for
387 loose to medium-dense sands. *Soils and Foundations* 56 (3), 460–472.
- 388 Vreugdenhil, R., Davis, R., Berrill, J., 1994. Interpretation of cone penetra-
389 tion results in multilayered soils. *International Journal for Numerical and*
390 *Analytical Methods in Geomechanics* 18 (9), 585–599.
- 391 Walker, J., Yu, H. S., 2010. Analysis of the cone penetration test in layered
392 clay. *Géotechnique* 60 (12), 939–948.
- 393 White, D. J., 2002. An investigation into the behaviour of pressed-in piles.
394 Ph.D. thesis, Cambridge University.
- 395 White, D. J., Bolton, M. D., 2004. Displacement and strain paths during
396 plane-strain model pile installation in sand. *Géotechnique* 54 (6), 375–397.
- 397 White, D. J., Take, W. A., Bolton, M. D., 2003. Soil deformation mea-
398 surement using particle image velocimetry (PIV) and photogrammetry.
399 *Géotechnique* 53 (7).

- 400 Xu, X. T., 2007. Investigation of the end bearing performance of displacement
401 piles in sand. Ph.D. thesis, The University of Western Australia.
- 402 Xu, X. T., Lehane, B. M., 2008. Pile and penetrometer end bearing resistance
403 in two-layered soil profiles. *Géotechnique* 58 (3), 187–197.
- 404 Youd, T. L., Idriss, I. M., 2001. Liquefaction resistance of soils: Summary
405 report from the 1996 NCEER and 1998 NCEER/NSF workshops on evalu-
406 ation of liquefaction resistance of soils. *Journal of Geotechnical and Geoen-*
407 *vironmental Engineering* 127 (4), 297–313.